

University of Nebraska - Lincoln

DigitalCommons@University of Nebraska - Lincoln

---

Biological Systems Engineering: Papers and Publications

Biological Systems Engineering

---

1-2020

## Field assessment of interreplicate variability from eight electromagnetic soil moisture sensors

Tsz Him Lo

Daran Rudnick


Jasreman Singh

Hope Njuki Nakabuye

Abia Katimbo

*See next page for additional authors*

Follow this and additional works at: <https://digitalcommons.unl.edu/biosysengfacpub>

 Part of the [Bioresource and Agricultural Engineering Commons](#), [Environmental Engineering Commons](#), and the [Other Civil and Environmental Engineering Commons](#)

---

This Article is brought to you for free and open access by the Biological Systems Engineering at DigitalCommons@University of Nebraska - Lincoln. It has been accepted for inclusion in Biological Systems Engineering: Papers and Publications by an authorized administrator of DigitalCommons@University of Nebraska - Lincoln.

---

**Authors**

Tsz Him Lo, Daran Rudnick, Jasreman Singh, Hope Njuki Nakabuye, Abia Katimbo, Derek M. Heeren, and Yufeng Ge

---

# Field assessment of interreplicate variability from eight electromagnetic soil moisture sensors

Tsz Him Lo, Daran R. Rudnick, Jasreman Singh,  
Hope Njuki Nakabuye, Abia Katimbo,  
Derek M. Heeren, & Yufeng Ge

Department of Biological Systems Engineering, University of Nebraska–Lincoln

*Corresponding author* — D. R. Rudnick, 402 West State Farm Road, North Platte, NE 69101, USA;  
*email* daran.rudnick@unl.edu

## Abstract

Interreplicate variability—the spread in output values among units of the same sensor subjected to essentially the same condition—can be a major source of uncertainty in sensor data. To investigate the interreplicate variability among eight electromagnetic soil moisture sensors through a field study, eight units of TDR315, CS616, CS655, HydraProbe2, EC5, 5TE, and Teros12 were installed at a depth of 0.30 m within 3 m of each other, whereas three units of AquaSpy Vector Probe were installed within 3 m of each other. The magnitude of interreplicate variability in volumetric water content ( $\theta_v$ ) was generally similar between a static period near field capacity and a dynamic period of 85 consecutive days in the growing season. However, a wider range of variability was observed during the dynamic period primarily because interreplicate variability in  $\theta_v$  increased sharply whenever infiltrated rainfall reached the sensor depth. Interreplicate variability for most sensors was thus smaller if comparing

---

Published in *Agricultural Water Management* 231 (2020), 105984.

doi: 10.1016/j.agwat.2019.105984

Copyright © 2019 Elsevier B.V. Used by permission.

Submitted 12 April 2019; revised 16 December 2019; accepted 16 December 2019.

The mention of trade names or commercial products is for the information of the reader and does not constitute an endorsement or recommendation for use by the authors or their institutions.

$\theta_v$  changes over several days that excluded this phenomenon than if comparing  $\theta_v$  directly. Among the sensors that also reported temperature and/or apparent electrical conductivity, the sensors exhibiting the largest interreplicate variability in these outputs were characterized by units with consistently above or below average readings. Although manufacturers may continue to improve the technology in and the quality control of soil moisture sensors, users would still benefit from paying greater attention to interreplicate variability and adopting strategies to mitigate the consequences of interreplicate variability.

**Keywords:** Apparent electrical conductivity, Precision, Soil water content, Standard deviation, Temperature, Uncertainty

## 1. Introduction

Soil moisture is an important property affecting the physics, chemistry, and biology of soils. In turn, moisture-driven changes in soil characteristics and processes affect the urban, agricultural, and natural ecosystems aboveground as well as local to global hydrological and meteorological cycles. Therefore, measuring soil moisture is of high interest for understanding and managing our world (Topp and Ferré, 2002).

The past century witnessed the development of electromagnetic (EM) sensors that can serve as relatively convenient and inexpensive tools for continuously measuring soil moisture at fixed depths in fixed locations. Concurrently, accompanying research revealed gradually that the permittivity-driven raw output of EM sensors does not exhibit the same relationship with volumetric soil water content ( $\theta_v$ ) in all environments (Topp et al., 2000). Because site-specific  $\theta_v$  calibration can be difficult and cost-prohibitive in many applications, studies have attempted to account for the influence of measurable soil properties (e.g., specific surface area, temperature (T), salinity, bulk density, organic matter content) on  $\theta_v$  calibrations using physically based dielectric mixing models (Dirksen and Dasberg, 1993; Or and Wraith, 1999; Schwartz et al., 2009) or empirical corrections (Jacobsen and Schjønning, 1993; Western and Seyfried, 2005; Kelleners et al., 2009b; Singh et al., 2019).

However, the influence of measurable soil properties is not the only source of error in  $\theta_v$  determination using EM sensors. Another source of error is interreplicate variability arising from inconsistencies in sensor hardware and/or from sensitivity to microscale differences. On one hand, the dimensions and EM behavior of sensor components may vary among different units of the same EM sensor. The same permittivity

consequently results in different output values. On the other hand, even under uniform management,  $\theta_v$  and/or other EM related soil properties may vary within the representative elementary volume (REV). If an EM sensor responds preferentially to the wetter zones (Logsdon, 2009) and/or measures a volume smaller than the REV, output values will vary among identical units of that sensor depending on the microscale spatial distribution of  $\theta_v$  and/or of other EM related soil properties. Although significant interreplicate variability can severely restrict the accuracy of EM sensors with and without site-specific calibration, this type of error has received relatively little attention (Evelt et al., 2006, 2009; Rosenbaum et al., 2010). Therefore, the objective of this study was to quantify the interreplicate variability of eight EM sensors under field conditions.

## **2. Methods**

### **2.1. Sensors**

The eight EM sensors in this study were TDR315 (Acclima, Meridian, ID), CS616 (Campbell Scientific, Logan, UT), CS655 (Campbell Scientific, Logan, UT), HydraProbe2 (HP2; Stevens Water, Portland, OR), EC5 (METER Group, Pullman, WA), 5TE (METER Group, Pullman, WA), Teros12 (METER Group, Pullman, WA), and Vector Probe (VP; AquaSpy, San Diego, CA). Each of these sensors measures a property that is related to soil permittivity, which in turn is positively associated with  $\theta_v$ . TDR315 is a time domain reflectometer that generates its own EM pulses and analyzes its own waveforms to obtain travel times (Schwartz et al., 2016). CS616 and CS655 are both water content reflectometers that count the average times per second the reflection of the previous generated EM pulse returns to the sensor head to trigger the next generated EM pulse (Seyfried and Murdock, 2001; Kelleners et al., 2005). However, CS655 also measures apparent electrical conductivity ( $EC_a$ ) to adjust factory calculations of apparent permittivity (Caldwell et al., 2018; Kargas and Soulis, 2019). HP2 is an impedance sensor that determines real and imaginary permittivities (Seyfried and Murdock, 2004; Kelleners et al., 2009a). EC5, 5TE, and Teros12 are capacitance sensors that use the surrounding soil as the dielectric of a capacitor in their circuitry and measure the charge times of this capacitor (Bogena et al., 2007; Kizito et al.,

2008; Rosenbaum et al., 2010, 2011). VP is a multisensor capacitance probe (Sloane, 2017) that reports scaled frequency at 0.10, 0.20, 0.30, 0.40, 0.50, 0.60, 0.70, 0.80, 0.90, 1.00, 1.10, and 1.20m depths.

## **2.2. Experiments**

This study was composed of two experiments that were conducted in a medium textured soil under no-till corn-soybean rotation at the University of Nebraska–Lincoln West Central Research and Extension Center in North Platte, NE. In the 2018 experiment, two side-by-side rectangular pits (i.e., the west pit and the east pit) were excavated 1.06m apart. Each pit was 1.83m long in the north-south direction by 0.46m wide in the east-west direction by 0.41m deep. In each horizontal (i.e., northwest, southwest, northeast, southeast) quadrant of each pit, one unit each of TDR315, CS616, CS655, HP2, EC5, 5TE, and Teros12 was inserted horizontally into the lengthwise (i.e., west/east) face of the pit at a depth of 0.30m until the base of the sensor head was flush with the pit wall. The sensor spacing along the length of each pit was 0.13 m, and all sensors except HP2 (whose prongs are not coplanar) were oriented such that all prongs were on the same horizontal plane. The excavated soil was carefully backfilled so that the sensor cables were bending downward from the sensor heads before bending upward to exit the pits and so that the top of each pit was neither a mound nor a depression. The four units of TDR315, CS616, CS655, HP2, EC5, and 5TE in each pit were connected to the same CR1000 datalogger (Campbell Scientific, Logan, UT) for recording sensor readings every 15 min. The four units of Teros12 in each pit were connected to the same EM60 G datalogger (METER Group, Pullman, WA) for recording sensor readings every 15 min and for uploading data every six hours to the manufacturer's website (<https://zentracloud.com>) via telemetry. While sensor installation occurred on March 14–15, planting occurred on May 10. Specifically, soybean seed product P25A12X (DuPont Pioneer, Johnston, IA) was planted by hand in 0.19m rows parallel with the length of the pits (i.e., along the north-south direction) at a seed spacing of 0.03m and at a depth of 0.03 m, and the previously removed corn residue was once again spread evenly over the site. The dense crop stand was intended to create a laterally homogeneous soil moisture distribution so that sensors with varying measurement volumes would be subjected to similar environments.

In the 2017 experiment, which was located 23m away from the 2018 experiment, soybean seed product 2511NRR (Hoegemeyer Hybrids, Hooper, NE) was mechanically planted on May 25 in 0.76m rows along the north-south direction at a seed spacing of 0.03m and at a depth of 0.05 m. On June 14, a total of three VPs were installed by the manufacturer in two adjacent crop rows such that the VPs formed the northwest, northeast, and southeast corners of a 3.0m long and 0.76m wide rectangle. The VPs were set up to record their sensor readings every 15 min and to upload those readings periodically to the manufacturer's website (<https://agspy.aquaspy.com>) via telemetry.

For comparison, a 503DR neutron moisture meter (NMM; CPN International, Concord, CA) was used in this study. From each corner of each pit in the 2018 experiment, an aluminum access tube was installed 0.30m outward in the lengthwise direction and 0.06m outward in the widthwise direction. In the 2017 experiment, a total of three aluminum access tubes were installed in the same two rows as the VPs such that the tubes formed the northwest, northeast, and southeast corners of a 2.1m long and 0.76m wide rectangle enclosed within the rectangle defined by the three VPs. In both experiments, NMM readings were always centered at the depths of the EM sensors and were always taken for a count duration of 16 s.

After the two experiments, two intact cylindrical soil cores of 0.04m diameter and 0.10m length centering at the sensor depth were collected for each sensor depth within the study areas using a hydraulic direct push soil probe (Giddings Machine Company, Windsor, CO). Textural composition and organic matter content were analyzed using the hydrometer and loss-on-ignition methods, respectively, by Ward Laboratories (Kearney, NE). The oven-dried weight of each core was divided by the original volume of that core to calculate bulk density. These soil properties were summarized in **Table 1**.

### **2.3. Analyses**

In this study, interreplicate variability was quantified in terms of the sample standard deviation (SD; Eq. 1). This definition lumps together the impacts of sensor hardware irregularities and of microscale soil heterogeneities. Because users tend to leave the EM sensors under investigation in place for at least one growing season but tend to carry the same

**Table 1.** Sand, silt, clay, organic matter (OM), and bulk density ( $\rho_b$ ) at the sensor depths of this study.

Depth (m)	2018				2017							
	0.30	0.20	0.30	0.40	0.50	0.60	0.70	0.80	0.90	1.00	1.10	1.20
Sand (%)	30	35	30	29	31	38	38	38	38	36	36	34
Silt (%)	41	38	41	41	41	37	35	36	36	38	39	39
Clay (%)	30	27	29	30	28	26	27	26	26	27	26	28
OM (%)	2.1	1.9	2.0	2.4	1.9	1.9	1.8	1.8	1.7	1.5	1.5	1.5
$\rho_b$ (g cm <sup>-3</sup> )	1.36	1.46	1.35	1.27	1.18	1.30	1.28	1.29	1.27	1.29	1.32	1.34

NMM unit between measurement locations, users decrease their uncertainty in sample means typically by increasing the number of EM sensor units or by increasing the number of NMM access tubes. Thus, the different units of the same EM sensor were treated as replicates of that EM sensor, whereas the different NMM access tubes in the same experiment were treated as replicates of NMM.

$$SD = \left[ \sum_{i=1}^n (X_i - X_{\bullet})^2 \div (n-1) \right]^{1/2} \quad (1)$$

where  $n$  = the number of replicates,  $i$  = the index for replicates,  $X_i$  = the variable of interest (i.e., T, EC<sub>a</sub>,  $\theta_v$ , cumulative  $\Delta\theta_v$ , or interval  $\Delta\theta_v$ ) as measured by replicate  $i$  of the given sensor at the given time, and  $X_{\bullet}$  = the interreplicate mean of the variable of interest for the given sensor at the given time.

The sole factory  $\theta_v$  calibration was applied to TDR315, CS655, 5TE, and NMM, respectively. In contrast, the standard quadratic calibration for CS616, the default loam calibration for HP2, the mineral soil calibration for EC5, and the mineral soil calibration for Teros12 were selected from multiple factory  $\theta_v$  calibrations. The manufacturer of the VP does not recommend any  $\theta_v$  calibration, but each deviation from the interreplicate mean in scaled frequency (0–100 %) was multiplied by 0.005 to convert to a deviation from the interreplicate mean in  $\theta_v$  (0–0.5 m<sup>3</sup>m<sup>-3</sup>) according to a graph of scaled frequency versus  $\theta_v$  from a manufacturer representative (Sloane, 2017).

A static assessment of interreplicate variability in  $\theta_v$  focused on four instances, coinciding with measurement dates of NMM, when the sensor depths were near field capacity and were not experiencing root water uptake. For TDR315, CS616, CS655, HP2, EC5, 5TE, Teros12, and NMM,



these four instances were on April 19, April 30, May 4, and May 10 (all before germination) in the 2018 experiment. Here, the static assessment SD in  $\theta_v$  for each of these sensors at each of the four dates included all eight replicates. For VP and NMM in the 2017 experiment, these four instances were on July 7, July 10, July 12, and July 14 (root water uptake was occurring at shallow depths only). Here, the static assessment SD in  $\theta_v$  for each of these sensors at each of the four dates included the equivalent of nine replicates, pooling together the deviations from depth-specific interreplicate means at the 1.00, 1.10, and 1.20m depths among all three replicates of VP or NMM.

A dynamic assessment of interreplicate variability in  $\theta_v$  incorporated all sensor readings from a continuous period of 85 days during the growing season. The period from May 11 to August 3 in the 2018 experiment included 18 NMM measurement times. For unknown reasons, all four replicates of EC5 in the east pit of the 2018 experiment began to report nonsensical  $\theta_v$  values from June 9 onward, so EC5 was excluded from the dynamic assessment. The dynamic assessment SD in  $\theta_v$  for TDR315, CS616, CS655, HP2, 5TE, Teros12, or NMM at any given time in 2018 included all eight replicates. On the other hand, the period from July 6 to September 28 in the 2017 experiment included 33 NMM measurement times. The dynamic assessment SD in  $\theta_v$  for VP or NMM at any given time in 2017 included all three replicates but was calculated separately at each of the 0.20, 0.30, 0.40, 0.50, 0.60, 0.70, 0.80, and 0.90m depths. In all cases, missing or zero values were omitted from SD calculations.

To some users, the magnitudes of changes in  $\theta_v$  ( $\Delta\theta_v$ ) are more important data than the actual values of  $\theta_v$ . Therefore, the interreplicate variability in two types of  $\Delta\theta_v$  was investigated for all sensors as a part of the dynamic assessment. The first type, cumulative  $\Delta\theta_v$ , was  $\Delta\theta_v$  from the first NMM measurement time to each of the latter measurement times. The second type, interval  $\Delta\theta_v$ , was  $\Delta\theta_v$  from each NMM measurement time (except for the last one) to the very next NMM measurement time. The 2018 and 2017 experiments included 17 and 32 intervals, respectively.

Some readers may be interested in how the factory calibrated results would change if adjusted using the local field thermogravimetric  $\theta_v$  calibration for the particular NMM unit, which achieved an  $R^2$  of 0.98 and a resubstitution root mean square error of  $0.010\text{m}^3\text{m}^{-3}$  with 54 soil cores from multiple depths. Specifically, SD values in  $\theta_v$  and in

$\Delta\theta_v$  for each sensor were multiplied by the linear regression slope that was obtained after averaging among all replicates and then plotting locally calibrated NMM  $\theta_v$  against factory calibrated  $\theta_v$  from the sensor of interest (**Table 2**). Although this adjustment was admittedly imperfect (Schwartz et al., 2018; Rudnick et al., 2018), developing accurate site-specific  $\theta_v$  calibrations of each EM sensor under investigation could not be accomplished given the authors' constraints. The adjusted results were arguably closer to reality than the factory calibrated results, but readers may choose to focus on the factory calibrated results and/or the adjusted results. The observed ranges in  $\theta_v$  by the NMM during this study are listed in **Table 3**.

Finally, some users depend on EM sensors to determine not only  $\theta_v$  but also T and  $EC_a$ . Among the eight EM sensors in this study, TDR315, CS655, HP2, 5TE, Teros12, and VP reported T, whereas TDR315, CS655, HP2, and 5TE reported  $EC_a$ . Thus, the interreplicate variability in T and in  $EC_a$  for these sensors was assessed according to the above methodology for the interreplicate variability in  $\theta_v$ . However, in both the static and the dynamic assessments of interreplicate variability in  $EC_a$ , SD from the 2018 experiment included just seven replicates. Specifically, the northwest quadrant of the east pit was excluded because the 5TE unit reported nonsensical  $EC_a$  values throughout the experiment for unknown reasons.

For clarity, a summary of this subsection and an outline of the following results and discussion section are provided in **Table 4**.

### 3. Results and discussion

#### 3.1. Static assessment

In the static assessment when the soil surrounding the sensors was near field capacity and was not experiencing root water uptake, all eight EM sensors under investigation exhibited larger interreplicate variability in factory and adjusted  $\theta_v$  as compared with NMM (**Table 5**). However, TDR315, CS655, VP, and NMM kept SD below  $0.020\text{m}^3\text{m}^{-3}$  on all four dates with and without adjustment. In contrast, HP2 exhibited relatively large interreplicate variability in factory and adjusted  $\theta_v$ , keeping SD above  $0.025\text{m}^3\text{m}^{-3}$  on all four dates. Adjustment changed the results noticeably for some sensors under evaluation. For example,

**Table 2.** Multiplicative adjustment factors—derived from the local thermogravimetric calibration for the neutron moisture meter (NMM) in this study—that were used to scale from factory calibrated results to adjusted results of standard deviation in  $\theta_v$  and in  $\Delta\theta_v$  for the sensors under investigation.

Sensor	NMM	TDR315	CS616	CS655	HP2	EC5	5TE	Teros12				
Adj.	1.28	1.12	1.06	0.99	1.10	1.76	2.07	1.30				
R <sup>2</sup>	N/A	0.98	0.95	0.98	0.99	0.94	0.95	0.98				
VP	0.20m	0.30m	0.40m	0.50m	0.60m	0.70m	0.80m	0.90m	1.00m	1.10m	1.20m	
Adj.	1.40	1.31	1.47	1.65	1.54	1.52	1.33	1.18	1.19	1.24	1.14	
R <sup>2</sup>	0.93	0.87	0.84	0.86	0.94	0.88	0.90	0.94	0.97	0.98	0.98	

**Table 3.** Ranges in volumetric water content ( $m^3m^{-3}$ )—according to the neutron moisture meter (NMM) using its local thermogravimetric calibration—among neutron moisture meter (NMM) measurement times for the static and dynamic assessments of this study.

	2018		2017							
Static	0.30m		1.00m		1.10m		1.20m			
$\theta_v$ Range	0.35-0.35		0.27-0.27		0.28-0.28		0.28-0.29			
	2018	2017								
Dynamic	0.30m	0.20m	0.30m	0.40m	0.50m	0.60m	0.70m	0.80m	0.90m	
$\theta_v$ Range	0.19-0.37	0.19-0.36	0.19-0.35	0.17-0.33	0.16-0.32	0.16-0.30	0.15-0.28	0.15-0.25	0.15-0.25	

**Table 4.** The order in which interreplicate variability results are presented in this paper and the number of replicates on which the assessment of each sensor was based for each variable of interest.

Sensor	2018								2017	
	NMM	TDR315	CS616	CS655	HP2	EC5	5TE	Teros12	NMM	VP
<b>Static Assessment</b>										
1. $\theta_v$	8	8	8	8	8	8	8	8	9*	9*
2. T	-	8	-	8	8	-	8	8	-	3
3. EC <sub>a</sub>	-	7	-	7	7	-	7	-	-	-
<b>Dynamic Assessment</b>										
4. T	-	8	-	8	8	-	8	8	-	3
5. EC <sub>a</sub>	-	7	-	7	7	-	7	-	-	-
6. $\theta_v$	8	8	8	8	8	-	8	8	3	3
7. cumul. $\Delta\theta_v$	8	8	8	8	8	-	8	8	3	3
8. interval $\Delta\theta_v$	8	8	8	8	8	-	8	8	3	3

\* 3 replicates each at 1.00, 1.10, and 1.20 m, respectively.

**Table 5.** Interreplicate standard deviation in factory calibrated volumetric water content ( $\theta_v$ ;  $\text{m}^3\text{m}^{-3}$ ), adjusted  $\theta_v$  ( $\text{m}^3\text{m}^{-3}$ ), temperature (T;  $^\circ\text{C}$ ), and apparent electrical conductivity ( $\text{EC}_a$ ;  $\text{dS m}^{-1}$ )—averaged among the four dates for the static assessment.

Sensor	2018								2017	
	NMM	TDR315	CS616	CS655	HP2	EC5	5TE	Teros12	NMM	VP
Factory $\theta_v$	0.010	0.013	0.022	0.017	0.027	0.017	0.012	0.015	0.009	0.013
Adj. $\theta_v$	0.013	0.014	0.023	0.017	0.030	0.031	0.025	0.020	0.012	0.016
T	N/A	1.3	N/A	0.2	0.2	N/A	0.2	0.3	N/A	0.5
$\text{EC}_a$	N/A	0.45	N/A	0.04	0.07	N/A	0.06	N/A	N/A	N/A

among the EM sensors, 5TE showed the smallest interreplicate variability in factory  $\theta_v$  but showed the third largest interreplicate variability in adjusted  $\theta_v$ .

The static assessment also examined interreplicate variability in T and  $\text{EC}_a$  (Table 5). CS655, HP2, and 5TE exhibited relatively small interreplicate variability in T, maintaining SD below  $0.4^\circ\text{C}$  on all four dates. On the other hand, CS655 showed the smallest interreplicate variability in  $\text{EC}_a$ , maintaining SD below  $0.05\text{ dSm}^{-1}$  on all four dates. The exceptionally large interreplicate variability in both T and  $\text{EC}_a$  for TDR315 was found to be characterized by substantial and persistent deviation of several replicates from the interreplicate mean. Specifically, the southwest and northeast replicates in the west pit and the southwest replicate in the east pit reported much higher T values than the mean, whereas the southeast replicate in the east pit reported much lower T values than the mean. On the other hand, the northwest replicate in the west pit and the northeast and southeast replicates in the east pit reported much higher  $\text{EC}_a$  values than the mean.

### 3.2. Dynamic assessment

#### 3.2.1. Temperature and apparent electrical conductivity

In agreement with the static assessment, the dynamic assessment found that interreplicate variability in T remained relatively small for CS655, HP2, 5TE, and Teros12 (**Fig. 1**). The 3<sup>rd</sup> quartile SD values of these four sensors were still lower than the minimum SD value for TDR315 even though the SD values for TDR315 were already smaller in the dynamic assessment than in the static assessment. Although the 1<sup>st</sup> quartile and median SD values were lowest for CS655, the range of SD values

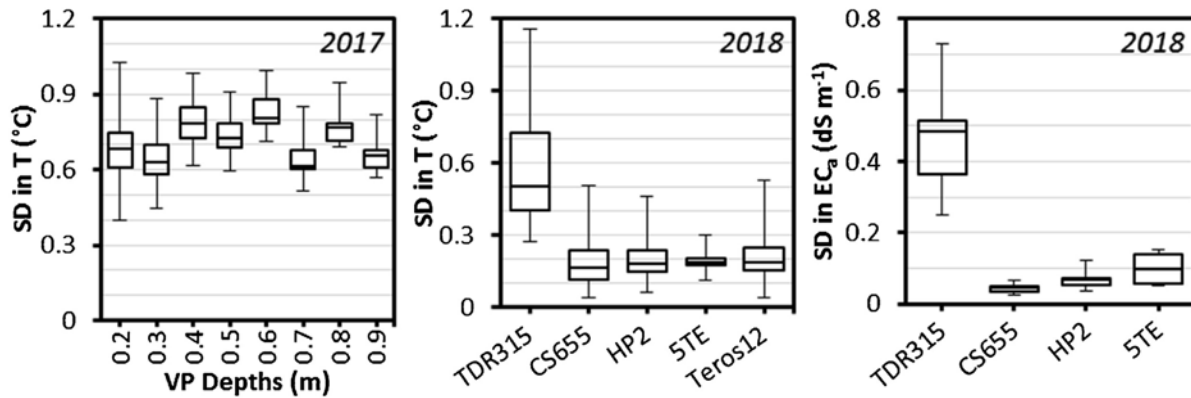


**Fig. 1.** Box-and-whisker plot of standard deviation values in temperature (T) and in apparent electrical conductivity (EC<sub>a</sub>) from 85 consecutive days of 15 min readings during the growing season.

was narrowest for 5TE, and almost all SD values for 5TE were below 0.3 °C. Interreplicate variability in T was relatively large for VP (Fig. 1) and—as identified earlier for TDR315—was also characterized by substantial and persistent deviation of particular replicates from the interreplicate mean. At the seven depths from 0.30m to 0.90 m, T was always highest for the southeast replicate and lowest for the northwest replicate.

Also in agreement with the static assessment, the dynamic assessment of interreplicate variability in EC<sub>a</sub> was the lowest for CS655 and highest for TDR315 (Fig. 1). Among the three core variables under investigation (i.e., T, EC<sub>a</sub>, and  $\theta_v$ ), the disparity between the most variable and least variable sensor was largest in EC<sub>a</sub>. The median, interquartile range, and total range of SD in EC<sub>a</sub> for TDR315 were all about 11 times those for CS655, with TDR315 being affected by substantial and persistent deviation of some replicates from the interreplicate mean as noted in the static assessment.

### 3.2.2. Volumetric water content

At the NMM measurement times during the 2018 dynamic assessment, TDR315, CS616, CS655, HP2, 5TE, and Teros12 all exhibited larger interreplicate variability in  $\theta_v$  as compared with NMM (Fig. 2). The 1<sup>st</sup> quartile SD values of these six EM sensors were higher than the 3<sup>rd</sup> quartile SD value of NMM with and without adjustment. Among these six EM sensors, the 1<sup>st</sup> quartile, median, and 3<sup>rd</sup> quartile SD values of TDR315 were among the lowest with and without adjustment. However, the

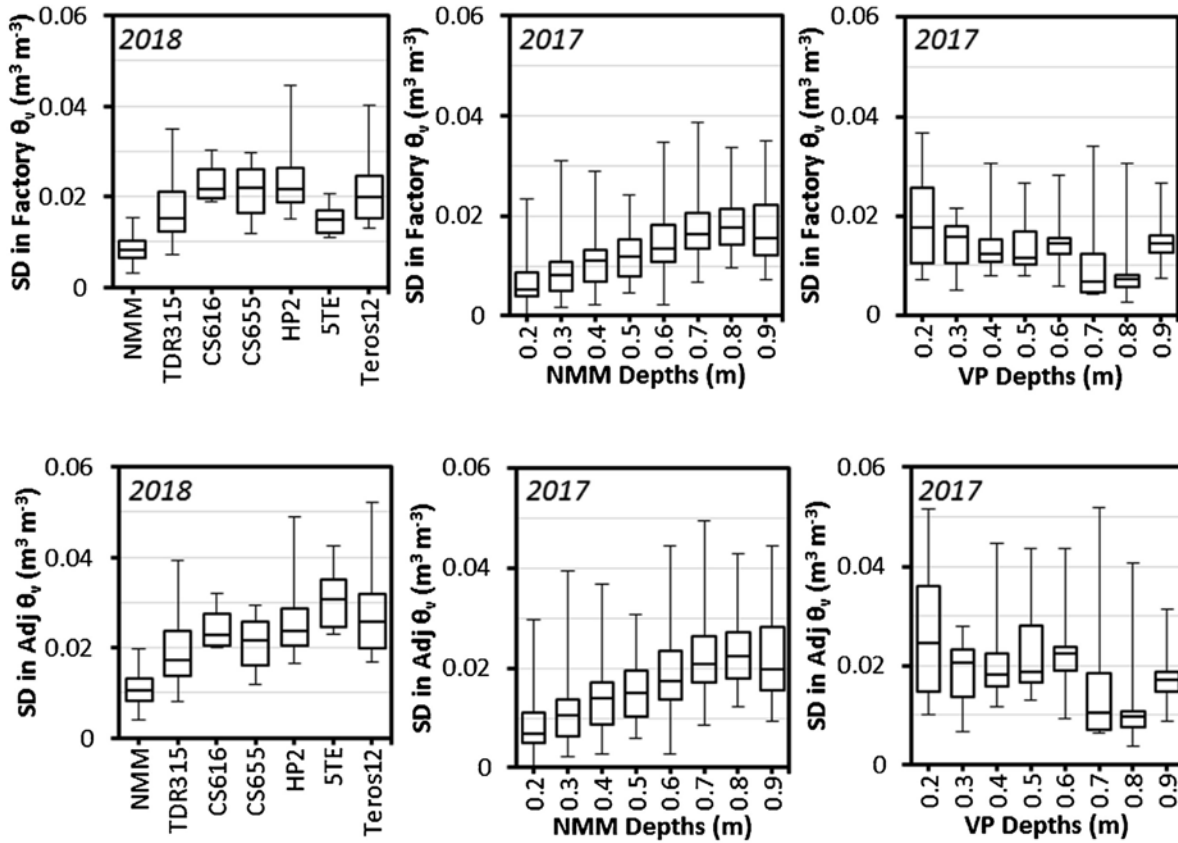


**Fig. 2.** Box-and-whisker plots of interreplicate standard deviation (SD) in factory and adjusted volumetric water content ( $\theta_v$ ) at the neutron moisture meter (NMM) measurement times for the dynamic assessment.

distribution of SD for TDR315 featured a relatively long upper tail, where maximum SD was  $0.039$  and  $0.035 \text{m}^3 \text{m}^{-3}$  with and without adjustment, respectively. SD values for HP2 and Teros12 also spanned relatively wide ranges. In contrast, all SD values for CS655 at the NMM measurement times stayed below  $0.030 \text{m}^3 \text{m}^{-3}$  with and without adjustment. Dynamic SD values were slightly higher than static SD values for CS655 and Teros12, while the reverse was true for HP2. Nonetheless, static and dynamic SD values in  $\theta_v$  were similar in magnitude overall based on the NMM measurement times in the 2018 experiment.

On the other hand, VP did not exhibit consistently larger interreplicate variability in  $\theta_v$  than NMM did at the NMM measurement times during the 2017 dynamic assessment (Fig. 2). At shallower depths with and without adjustment, SD values for VP were generally higher than those

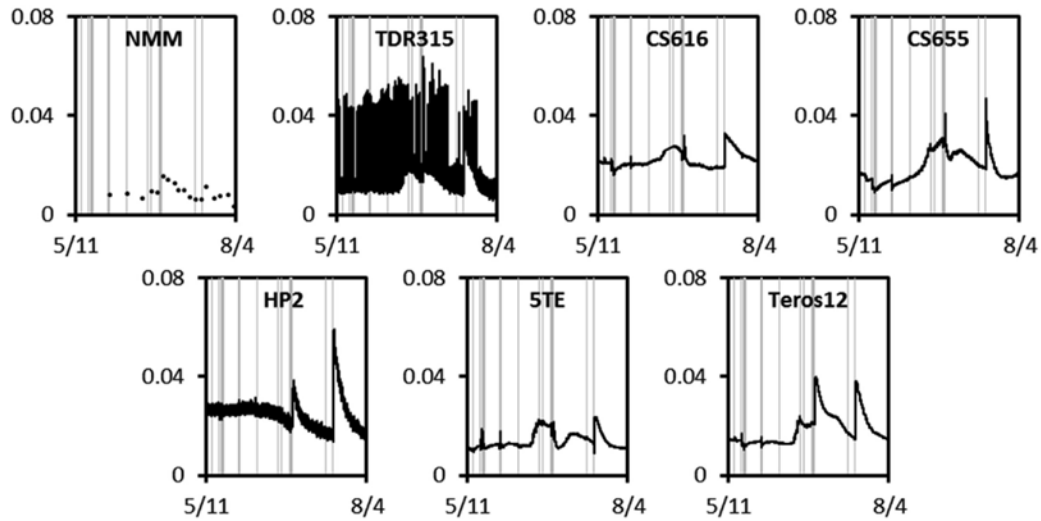
for NMM. The opposite, however, tended to be true at deeper depths as SD values for NMM clearly increased with increasing depth. For both VP and NMM, adjusted SD values spanned a range wider than  $0.03\text{m}^3\text{m}^{-3}$  at most depths. A smaller number of replicates (i.e., three as opposed to eight) but a larger number of NMM measurement times (i.e., 33 as opposed to 18) likely contributed to the greater diversity in SD values during the 2018 dynamic assessment as compared with during the 2017 dynamic assessment.

The effects of wetting and drying on interreplicate variability in  $\theta_v$  were examined from the entire 85 day time series (**Fig. 3**). Both for the EM sensors under investigation and for NMM, rain events that increased  $\theta_v$  triggered jumps in its SD. This behavior was likely caused by microscale nonuniformity in effective precipitation and subsequent percolation (i.e., preferential flow as opposed to piston flow). On the other hand, drying sequences generally preserved or steadily decreased SD, but sometimes replicates drifted apart as drying continued. Perhaps the rate and vertical distribution of root water uptake around the replicates were gradually diverging. Such drifting was found in the 1<sup>st</sup> quarter of the 2017 dynamic assessment at all VP and NMM depths except for 0.20 m. In the 2<sup>nd</sup> quarter of the 2018 dynamic assessment, various extents of such drifting were found for TDR315, CS616, CS655, 5TE, and Teros12 but not for HP2 and NMM. Rises in SD due to replicates drifting apart were not as abrupt as those due to percolating rainfall, but the former was still observed to roughly double SD values for VP and NMM in 2017 and for CS655 in 2018. The time series graphs revealed additionally that TDR315 and HP2 experienced obvious fluctuations in  $\theta_v$  readings. From one reading to another 15 min apart, TDR315 showed sudden and erratic spikes in  $\theta_v$  whereas HP2 oscillated constantly. Filtering and smoothing procedures could be employed to enhance data precision amidst the noise.

### 3.2.3. Change in volumetric water content

Examining the interreplicate variability in  $\Delta\theta_v$  would not only generate practical information to some users but also shed light into the nature of the interreplicate variability in  $\theta_v$ . If interreplicate variability in the starting value of  $\theta_v$  was the overwhelming reason for interreplicate variability in  $\theta_v$ , SD values in cumulative  $\Delta\theta_v$  would be much smaller than SD values in  $\theta_v$ . Median SD values in adjusted cumulative  $\Delta\theta_v$  were 0.010 and  $0.006\text{m}^3\text{m}^{-3}$  smaller than median SD values in adjusted  $\theta_v$  for





2017 Experiment

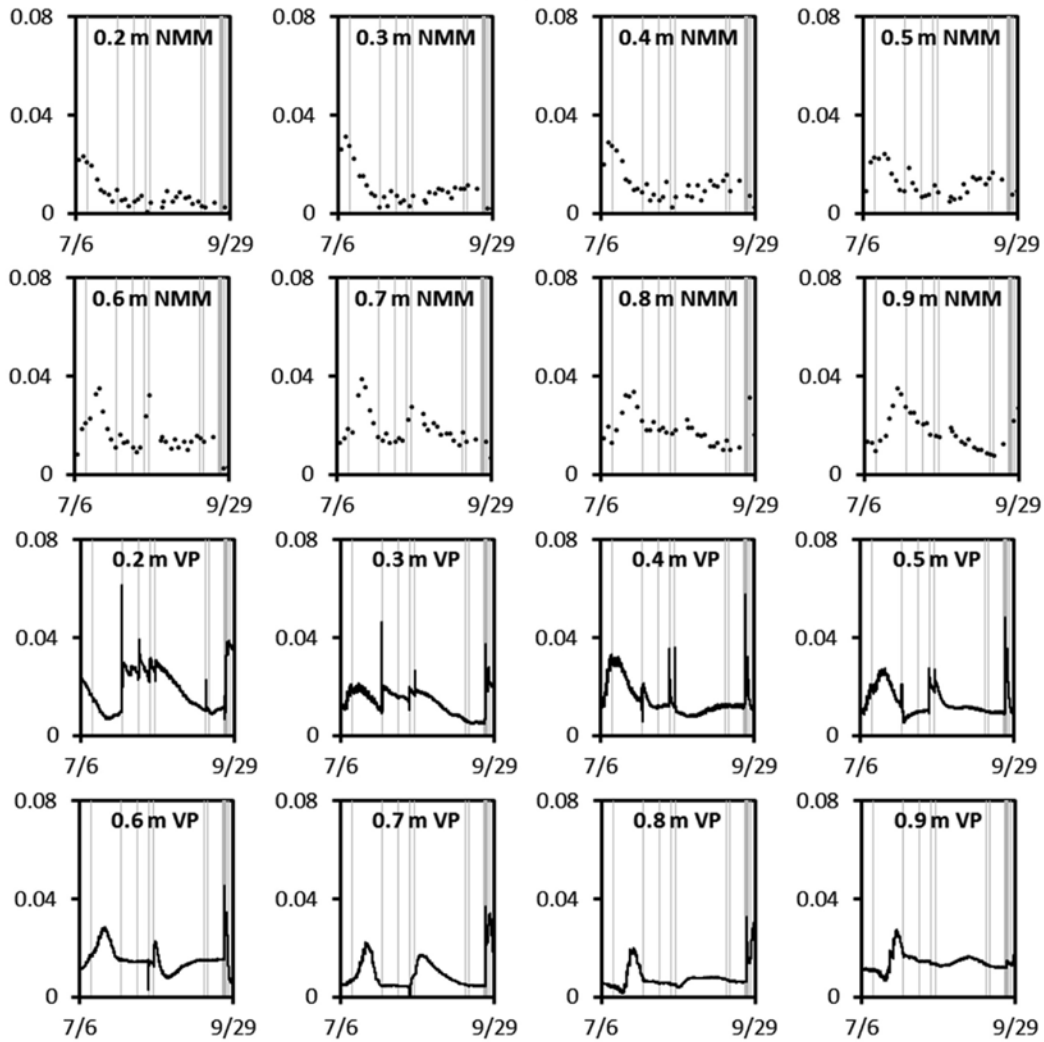




**Fig. 3.** Temporal trends of interreplicate standard deviation in factory volumetric water content ( $m^3m^{-3}$ ) over 85 consecutive days during the growing season; each grey vertical line denotes a 12 h interval with at least 5mm of rainfall according to the North Platte 3SW weather station (Nebraska State Climate Office, personal communication).

CS616 and CS655, respectively (**Figs. 2 and 4**). However, minimal reductions were observed for other sensors in the 2018 experiment. SD values in cumulative  $\Delta\theta_v$  were smaller than SD values in  $\theta_v$  at some depths for VP and NMM in the 2017 experiment, whereas the opposite was true at some other depths. For NMM in the 2017 experiment, SD values in cumulative  $\Delta\theta_v$  did not increase with increasing depth as SD values in  $\theta_v$  did. The lack of consistently smaller SD values in cumulative  $\Delta\theta_v$  than in  $\theta_v$  revealed that differences in the starting value of  $\theta_v$  were not the dominant source of interreplicate variability during the 2018 and 2017

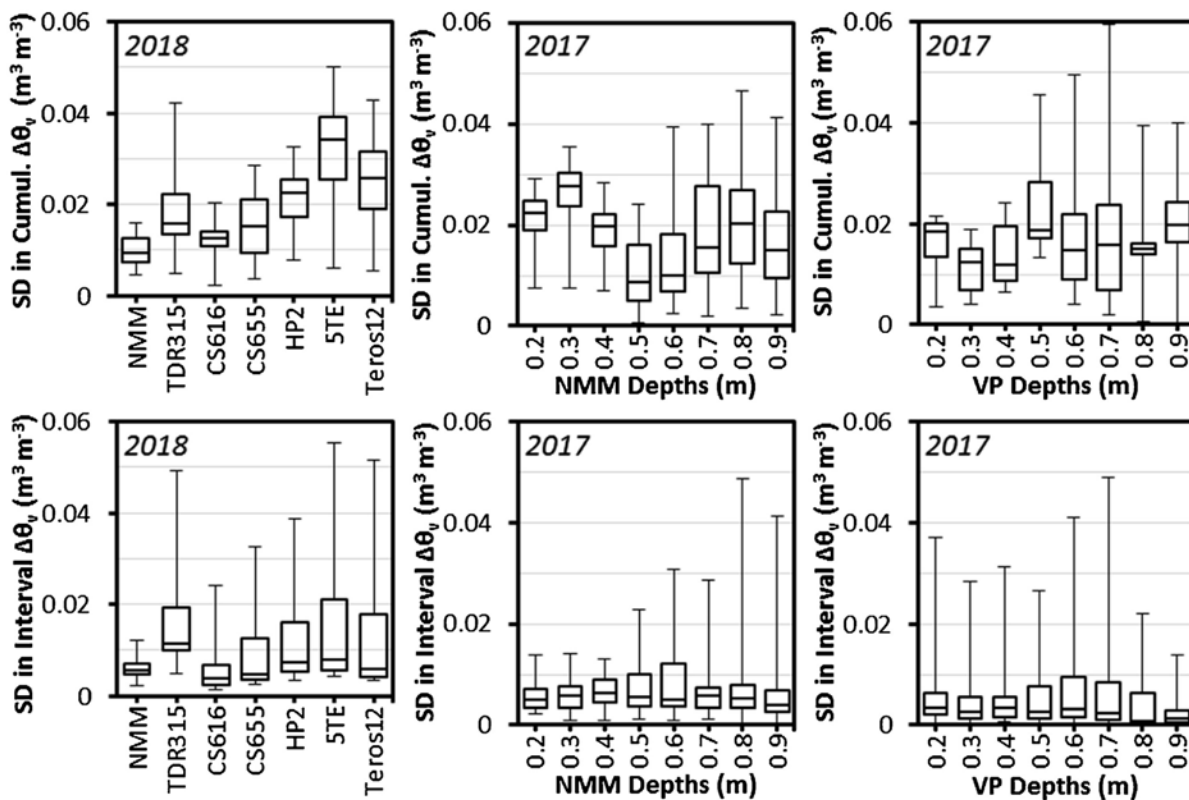


**Fig. 4.** Box-and-whisker plots of interreplicate standard deviation (SD) in cumulative and interval changes in adjusted volumetric water content ( $\Delta\theta_v$ ) at the neutron moisture meter (NMM) measurement times for the dynamic assessment.

dynamic assessments. The close proximity of all replicates in this study was expected to reduce the observed magnitude of spatial variability in initial  $\theta_v$  as compared with arrangements that scattered the replicates across a field. At the same time, divergences among replicates in effective precipitation, root water uptake, and/or sensor responses prevented the interreplicate differences in  $\theta_v$  from remaining constant throughout the dynamic assessment.

In contrast, interreplicate variability in  $\Delta\theta_v$  over short intervals of approximately 2–7 days was substantially smaller than interreplicate variability in  $\theta_v$  for all sensors except TDR315 (Figs. 2 and 4). The majority of SD values in adjusted interval  $\Delta\theta_v$  were below  $0.01\text{m}^3\text{m}^{-3}$ , and the SD values for CS616 and VP were mostly comparable to those for NMM. Nevertheless, a strong right skew in the distribution of SD values was especially prevalent among EM sensors. Those relatively large SD values corresponded to the intervals that included or immediately followed infiltration to the sensor depths, which was associated earlier with increases in interreplicate variability.

#### 4. Implications

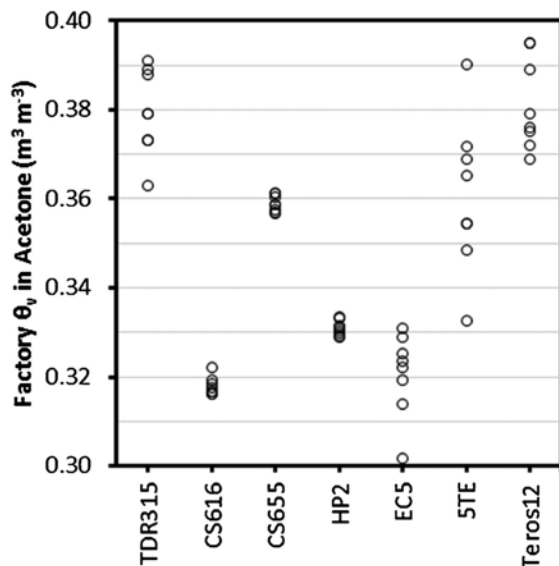
Soil moisture sensors are undoubtedly useful, but interreplicate variability poses a genuine challenge to the quantitative use of soil moisture sensor data. Even if the calibration is perfect, large interreplicate variability still prevents users from obtaining a confident value of T,  $\text{EC}_a$ , or  $\theta_v$  without deploying many replicates. In turn, data errors resulting from interreplicate variability of soil moisture sensors may propagate to the models to which users supply this data and to the decisions that users make based on this data.

To reduce interreplicate variability, inconsistency in sensor hardware should first be minimized through improved construction. Manufacturers can choose better parts and procedures that cause greater uniformity and durability in the mechanical and electrical characteristics affecting EM signal generation, transmission, reception, and interpretation. The inevitably remaining variability in sensor hardware can then be compensated through laboratory standardization of each individual unit (Rosenbaum et al., 2010) during factory calibration. Finally, internal and external damage to sensor hardware may occur after the product leaves the manufacturer (i.e., during shipping, installation, usage,

removal, and storage), so users must be on the alert for obvious physical deformities and for nonsensical data to decide when sensor repair or replacement is necessary.

Under field conditions, microscale differences in actual  $\theta_v$  and in soil properties that alter the relationship between  $\theta_v$  and sensor output cannot be completely eliminated. Therefore, users desiring precision in exact  $\theta_v$  are recommended to select soil moisture sensors that have been shown to exhibit small interreplicate variability and to be cautious of sensors that are by design (e.g., operating physical principles, EM frequency, EM field uniformity) predisposed to high sensitivity to microscale differences (Evetts et al., 2006, 2009). Furthermore, such users are advised to maximize the number of replicates under their particular labor and financial constraints and to avoid instantaneous, unfiltered data.

Differentiating the contribution of hardware inconsistency versus microscale heterogeneity on interreplicate variability among the EM sensors was impossible using only the 2017 and 2018 field experiments data. Therefore, eight replicates of TDR315, CS616, CS655, HP2, EC5, 5TE, and Teros12 were immersed one at a time in 10 °C acetone (Sunnyside Corporation, Wheeling, IL) indoors on October 30, 2019. Acetone served as a suitable reference liquid because it is easily accessible, is not overly hazardous, and maintains a similar permittivity within the



range of frequencies that are employed by the EM sensors under evaluation. VP was excluded from this laboratory test because no replicates were available. For the other seven EM sensors, the factory calibrated  $\theta_v$  from a particular replicate was recorded once the entire measurement volume of that replicate was inside acetone (Fig. 5).

**Fig. 5.** Factory calibrated volumetric water content ( $\theta_v$ ; m<sup>3</sup>m<sup>-3</sup>) from eight replicates of each sensor in 10 °C acetone.

Regrettably, the eight replicates in this laboratory test could not be guaranteed to be exactly the same eight replicates in the 2018 field experiment. Therefore, the results could not be applied to analyze further any systematic deviations from the interreplicate mean (i.e., whether a replicate that was routinely above/below average in the field was above/below average in acetone) or to isolate definitively the sensor hardware effect from the microscale heterogeneity effect. Furthermore, readers must not overgeneralize results from eight replicates. Nevertheless, interreplicate SD in factory  $\theta_v$  for acetone was loosely compared to interreplicate SD in factory  $\theta_v$  for the 2018 static assessment because the  $\theta_v$  corresponding to the permittivity of acetone is similar to  $\theta_v$  during the 2018 static assessment.

According to the interreplicate variability of the EM sensors in acetone, hardware variability was low for CS616, CS655, and HP2; moderate for TDR315, EC5, and Teros12; and high for 5TE (**Table 6**). On one hand, the high acetone:static ratio for TDR315 suggests that the potential for reducing its interreplicate variability lies predominantly in improving hardware consistency. On the other hand, the low acetone:static ratio for HP2 suggests that the potential for reducing its interreplicate variability lies predominantly in lowering sensitivity to microscale heterogeneity. Such sensitivity of HP2 may be related to its small and concentrated measurement volume, implying that spatial precision and interreplicate variability might sometimes be tradeoffs that need to be weighed depending on application. After all, interreplicate variability is only one of many important considerations. The user is ultimately responsible for selecting 1) the most scientifically and practically appropriate soil moisture sensors for a particular application, 2) the most optimal placement of those sensors given 3-D soil heterogeneity, and 3) the most reasonable approach to interpreting and using soil moisture data while accounting for the reality of interreplicate variability.

**Table 6.** Interreplicate standard deviation (SD) in factory calibrated volumetric water content ( $\text{m}^3\text{m}^{-3}$ ) for acetone and the ratio between the SD for acetone and SD for the static field assessment.

<i>Sensor</i>	<i>TDR315</i>	<i>CS616</i>	<i>CS655</i>	<i>HP2</i>	<i>EC5</i>	<i>5TE</i>	<i>Teros12</i>
Acetone ( $\text{m}^3\text{m}^{-3}$ )	0.010	0.002	0.002	0.002	0.009	0.017	0.010
Acetone:Static Ratio	0.77	0.09	0.11	0.06	0.53	1.41	0.69

Users who do not absolutely require the knowledge of  $\theta_v$  itself, however, may wish to reduce their exclusive reliance on the exact  $\theta_v$  reading from soil moisture sensors. For example, many irrigated agronomic crop producers who use soil moisture sensors monitor multiple depths at just one location per field. Without replication, scheduling irrigation strictly based on a fixed  $\theta_v$  threshold would be difficult even in the absence of calibration error because SD values in  $\theta_v$  of  $0.02\text{m}^3\text{m}^{-3}$ , which were commonly observed in this study, are approximately between an eighth and a quarter of available water capacity in most soils. Additionally, based on the overall similarity between SD values in  $\theta_v$  and SD values in cumulative  $\Delta\theta_v$  for the sensors in this study, it might not be easier to schedule irrigation strictly based on a fixed cumulative  $\Delta\theta_v$  threshold relative to an observational field capacity (Lo et al., 2017) value that is defined early in the season. This study suggests that the interreplicate variability for soil moisture sensors should not be blindly assumed to consist mostly of constant offsets persisting throughout the growing season.

From their experiences in this study and from their interactions with producers and industry, the authors have discerned the need to further research unconventional irrigation scheduling approaches that focus on the drying sequences in EM sensor data and integrate multiple data sources. For instance, at the beginning of each drying sequence, field capacity at each thoroughly wetted depth might be redefined as the output value corresponding to the end of nonlinear or nighttime decline (Starr and Paltineanu, 1998). Subsequently, the roughly linear and stair step-like daytime decline across depths might be related either to a known calibration or to expected rates of crop water use (Thompson et al., 2007). Finally, a comparison of active extraction depth against expected effective rooting depth (T. G. Smith, personal communication, 2014) and a comparison of current profile depletion against profile allowable depletion (Merriam, 1966) might be jointly considered to make irrigation decisions. By depending on the ability of EM sensors mainly to describe  $\theta_v$  trends and to quantify  $\Delta\theta_v$  within each drying sequence (Starr and Paltineanu, 1998; Singh et al., 2018), such an approach might be more accommodating of shortcomings in calibration and/or interreplicate variability. Future field studies that implement and evaluate this type of approach as well as complex ensemble approaches combining soil moisture sensing, soil water balance

modeling, and thermal sensing/energy balance modeling (Barker et al., 2018) would be greatly welcomed to overcome the challenge of relying solely on soil moisture sensor data.

**Declaration of interests** — No competing interests to declare.

**Acknowledgments** — This study was jointly supported by the National Institute of Food and Agriculture, U.S. Department of Agriculture (USDA-NIFA), under award number 2016-68007-25066, “Sustaining agriculture through adaptive management to preserve the Ogallala aquifer under a changing climate”; by USDA-NIFA under award number 2017-68007-26584, “Securing water for and from agriculture through effective community and stakeholder engagement”; by USDA-NIFA under Hatch Project #1015698, “Integrating hydrological modeling and characterization approaches across scales to understand the effects of efficient irrigation management on groundwater/surface water systems”; by Nebraska Extension; and by the Daugherty Water for Food Global Institute. The authors are grateful to METER Group for donating Teros12 sensors; to AquaSpy, Inc., and Frenchman Valley Cooperative for lending out Vector Probes; and to Nebraska State Climate Office for providing weather data from its Nebraska Mesonet. The authors thank Turner Dorr, Jacob Nickel, Deepti Upadhyaya, and Italo Pinho de Faria for assisting this study.

## References

- Barker, J.B., Heeren, D.M., Neale, C.M.U., Rudnick, D.R., 2018. Evaluation of variable rate irrigation using a remote-sensing-based model. *Agric. Water Manag.* 203, 63–74. <https://doi.org/10.1016/j.agwat.2018.02.022>
- Bogena, H.R., Huisman, J.A., Oberdörster, C., Vereecken, H., 2007. Evaluation of a low-cost soil water content sensor for wireless network applications. *J. Hydrol.* 344 (1–2), 32–42. <https://doi.org/10.1016/j.jhydrol.2007.06.032>
- Caldwell, T.G., Bongiovanni, T., Cosh, M.H., Halley, C., Young, M.H., 2018. Field and laboratory evaluation of the CS655 soil water content sensor. *Vadose Zone J.* 17 (1), 170214. <https://doi.org/10.2136/vzj2017.12.0214>
- Dirksen, C., Dasberg, S., 1993. Improved calibration of time domain reflectometry soil water content measurements. *Soil Sci. Soc. Am. J.* 57 (3), 660–667. <https://doi.org/10.2136/sssaj1993.03615995005700030005x>
- Evett, S.R., Schwartz, R.C., Tolk, J.A., Howell, T.A., 2009. Soil profile water content determination: spatiotemporal variability of electromagnetic and neutron probe sensors in access tubes. *Vadose Zone J.* 8 (4), 926–941. <https://doi.org/10.2136/vzj2008.0146>
- Evett, S.R., Tolk, J.A., Howell, T.A., 2006. Soil profile water content determination: sensor accuracy, axial response, calibration, temperature dependence, and precision. *Vadose Zone J.* 5 (3), 894–907. <https://doi.org/10.2136/vzj2005.0149>



- Jacobsen, O.H., Schjønning, P., 1993. A laboratory calibration of time domain reflectometry for soil water measurement including effects of bulk density and texture. *J. Hydrol. (Amst)* 151 (2–4), 147–157. [https://doi.org/10.1016/0022-1694\(93\)90233-Y](https://doi.org/10.1016/0022-1694(93)90233-Y)
- Kargas, G., Soulis, K.X., 2019. Performance evaluation of a recently developed soil water content, dielectric permittivity, and bulk electrical conductivity electromagnetic sensor. *Agric. Water Manag.* 213, 568–579. <https://doi.org/10.1016/j.agwat.2018.11.002>
- Kelleners, T.J., Seyfried, M.S., Blonquist, J.M., Bilskie, J., Chandler, D.G., 2005. Improved interpretation of water content reflectometer measurements in soils. *Soil Sci. Soc. Am. J.* 69 (6), 1684–1690. <https://doi.org/10.2136/sssaj2005.0023>
- Kelleners, T.J., Ferre-Pikal, E.S., Schaap, M.G., Paige, G.B., 2009a. Calibration of hydra impedance probes using electrical circuit theory. *Soil Sci. Soc. Am. J.* 73 (2), 453–465. <https://doi.org/10.2136/sssaj2008.0151>
- Kelleners, T.J., Paige, G.B., Gray, S.T., 2009b. Measurement of the dielectric properties of Wyoming soils using electromagnetic sensors. *Soil Sci. Soc. Am. J.* 73 (5), 1626–1637. <https://doi.org/10.2136/sssaj2008.0361>
- Kizito, F., Campbell, C.S., Campbell, G.S., Cobos, D.R., Teare, B.L., Carter, B., Hopmans, J.W., 2008. Frequency, electrical conductivity and temperature analysis of a low-cost capacitance soil moisture sensor. *J. Hydrol.* 352 (3–4), 367–378. <https://doi.org/10.1016/j.jhydrol.2008.01.021>
- Lo, T., Heeren, D.M., Mateos, L., Luck, J.D., Martin, D.L., Miller, K.A., Barker, J.B., Shaver, T.M., 2017. Field characterization of field capacity and root zone available water capacity for variable rate irrigation. *Appl. Eng. Agric.* 33 (4), 559–572. <https://doi.org/10.13031/aea.11963>
- Logsdon, S.D., 2009. CS616 calibration: field versus laboratory. *Soil Sci. Soc. Am. J.* 73 (1), 1–6. <https://doi.org/10.2136/sssaj2008.0146>
- Merriam, J.L., 1966. A management control concept for determining the economical depth and frequency of irrigation. *Trans. ASAE* 9 (4), 492–498. <https://doi.org/10.13031/2013.40014>
- Or, D., Wraith, J.M., 1999. Temperature effects on soil bulk dielectric permittivity measured by time domain reflectometry: a physical model. *Water Resour. Res.* 53 (2), 371–383. <https://doi.org/10.1029/1998WR900008>
- Rosenbaum, U., Huismna, J.A., Vrba, J., Vereecken, H., Bogena, H.R., 2011. Correction of temperature and electrical conductivity effects on dielectric permittivity measurements with ECH<sub>2</sub>O sensors. *Vadose Zone J.* 10 (2), 582–593. <https://doi.org/10.2136/vzj2010.0083>
- Rosenbaum, U., Huisman, J.A., Weuthen, A., Vereecken, H., Bogena, H.R., 2010. Sensor-to-sensor variability of the ECH<sub>2</sub>O EC-5, TE, and 5TE sensors in dielectric liquids. *Vadose Zone J.* 9 (1), 181–186. <https://doi.org/10.2136/vzj2009.0036>
- Rudnick, D.R., Lo, T., Singh, J., Werle, R., Muñoz-Arriola, F., Shaver, T.M., Burr, C.A., Dorr, T.J., 2018. Reply to comments on “performance assessment of factory and field calibrations for electromagnetic sensors in a loam soil”. *Agric. Water Manag.* 203, 272–276. <https://doi.org/10.1016/j.agwat.2018.02.036>

- Schwartz, R.C., Evett, S.R., Anderson, S.K., Anderson, D.J., 2016. Evaluation of a direct-coupled time-domain reflectometry for determination of soil water content and bulk electrical conductivity. *Vadose Zone J.* 15 (1). <https://doi.org/10.2136/vzj2015.08.0115>
- Schwartz, R.C., Evett, S.R., Bell, J.M., 2009. Complex permittivity model for time domain reflectometry soil water content sensing: II. Calibration. *Soil Sci. Soc. Am. J.* 73 (3), 898–909. <https://doi.org/10.2136/sssaj2008.0195>
- Schwartz, R.C., Evett, S.R., Lascano, R.J., 2018. Comments on “performance assessment of factory and field calibrations for electromagnetic sensors in a loam soil”. *Agric. Water Manag.* 203, 236–239. <https://doi.org/10.1016/j.agwat.2018.02.029>
- Seyfried, M.S., Murdock, M.D., 2001. Response of a new soil water sensor to variable soil, water content, and temperature. *Soil Sci. Soc. Am. J.* 65 (1), 28–34. <https://doi.org/10.2136/sssaj2001.65128x>
- Seyfried, M.S., Murdock, M.D., 2004. Measurement of soil water content with a 50-MHz soil dielectric sensor. *Soil Sci. Soc. Am. J.* 68 (2), 394–403. <https://doi.org/10.2136/sssaj2004.3940>
- Singh, J., Lo, T., Rudnick, D.R., Dorr, T.J., Burr, C.A., Werle, R., Shaver, T.M., Muñoz-Arriola, F., 2018. Performance assessment of factory and field calibrations for electromagnetic sensors in a loam soil. *Agric. Water Manag.* 196, 87–98. <https://doi.org/10.1016/j.agwat.2017.10.020>
- Singh, J., Lo, T., Rudnick, D.R., Irmak, S., Blanco-Canqui, H., 2019. Quantifying and correcting for clay content effects on soil water measurement by reflectometers. *Agric. Water Manag.* 216, 390–399. <https://doi.org/10.1016/j.agwat.2019.02.024>
- Sloane, D., 2017. AquaSpy: Soil Moisture Sensors. Retrieved from. <http://map.northplainsgcd.org/master-irrigator/docs/sloane-part1.pdf>
- Starr, J.L., Paltineanu, I.C., 1998. Real-time soil water dynamics over large areas using multisensor capacitance probes and monitoring system. *Soil Tillage Res.* 47 (1–2), 43–49. [https://doi.org/10.1016/S0167-1987\(98\)00071-3](https://doi.org/10.1016/S0167-1987(98)00071-3)
- Thompson, R.B., Gallardo, M., Valdez, L.C., Fernández, M.D., 2007. Determination of lower limits for irrigation management using in situ assessments of apparent crop water uptake made with volumetric soil water content sensors. *Agric. Water Manag.* 92 (1–2), 13–28. <https://doi.org/10.1016/j.agwat.2007.04.009>
- Topp, G.C., Ferré, P.A., 2002. Water content. In: Dane, J.H., Topp, G.C. (Eds.), *Methods of Soil Analysis Part 4: Physical Methods*. Soil Science Society of America, Madison, WI, pp. 417–545. <https://doi.org/10.2136/sssabookser5.4.c19>
- Topp, G.C., Zegelin, S., White, I., 2000. Impacts of the real and imaginary components of relative permittivity on time domain reflectometry measurements in soils. *Soil Sci. Soc. Am. J.* 64 (4), 1244–1252. <https://doi.org/10.2136/sssaj2000.6441244x>
- Western, A.W., Seyfried, M.S., 2005. A calibration and temperature correction procedure for the water-content reflectometer. *Hydrol. Process.* 19 (18), 3785–3793. <https://doi.org/10.1002/hyp.6069>